International Journal of Computer Science and Information Technology
ISSN: 3005-9682 (Print), ISSN: 3005-7140 (Online) | Volume 3, Number 2, Year 2024
DOI: https://doi.org/10.62051/ijcsit.v3n2.42
Journal homepage: https://wepub.org/index.php/IJCSIT/index

Attitude Calculation Algorithm for Quadrotor UAV Based on Acceleration Correction Model

Hongbo Fan *

Department of Electronic Information Engineering, China West Normal University, Nanchong, Sichuan, China

*Corresponding Author: fhb1498660510@gmail.com

ABSTRACT

To enhance the accuracy of quadrotor UAV navigation systems in dynamic environments, we propose an attitude calculation method based on an acceleration correction model. This model estimates and corrects non-gravitational acceleration from the accelerometer, reducing its impact on attitude calculation. Experimental results demonstrate that this algorithm effectively mitigates non-gravitational acceleration interference and significantly improves the accuracy and anti-interference capability of UAV navigation systems.

KEYWORDS

Component; Quadroto UAV; Attitude calculation; Accelerometer; Kalman filtering

1. INTRODUCTION

Multirotor UAVs are vital in fields like aerial photography, irrigation, and surveying due to their low cost and high maneuverability. Accurate and real-time attitude estimation is crucial for UAV mission success. Low-cost UAVs typically use MEMS sensors, which are sensitive to non-gravitational accelerations, causing significant errors in dynamic environments. This study proposes an attitude estimation algorithm based on an acceleration correction model to enhance accuracy and stability in dynamic conditions.

2. LITERATURE REVIEW

Reference [1] uses a direction cosine matrix combined with complementary filtering for attitude updates, aiming to improve system accuracy. However, it is limited in dynamic environments with non-gravitational accelerations. Reference [2] designs a suppression function for non-gravitational acceleration using accelerometer and gyroscope data, showing good anti-interference but lacking precise estimation. Reference [3] employs an extended Kalman filter (EKF) with GPS and Doppler velocity log (DVL) for underwater vehicles, but its application in quadrotor UAVs is limited. Reference [4] proposes adaptive estimation and correction of non-gravitational acceleration, maintaining accuracy over short periods. Reference [5] uses GPS and airspeed indicators to correct non-gravitational acceleration, achieving accurate attitude representation but is limited by low update frequencies. Reference [6] combines GPS and inertial navigation systems (INS) with EKF for real-time position and attitude, requiring high GPS accuracy and stability, often needing costly differential GPS. In low-cost UAVs, single-point GPS has lower accuracy and slower updates, leading to significant attitude errors in GPS/INS combined algorithms.

Content from this work may be used under the terms of CC BY-NC 4.0 licence (https://creativecommons.org/licenses/by-nc/4.0/).
Published by Warwick Evans Publishing.

3. METHOD

3.1. UAV Attitude Modeling

3.1.1. Establishing the Coordinate System

The "North-East-Down" geographic coordinate system is chosen as the navigation frame (n-frame), and the "Forward-Right-Down" coordinate system is used as the body frame (b-frame). The n-frame is orthogonal relative to the Earth's horizontal plane, with X_n, Y_n and Z_n axes pointing north, east, and down. The b-frame is fixed to the UAV with X, Y and$Z$axes pointing forward, right, and down. The transformation matrix from the n-frame to the b-frame is represented by the direction cosine matrix:

$$C_n^b = \begin{pmatrix} \cos\theta\cos\psi & \cos\theta\sin\psi & -\sin\theta \\ \cos\psi\sin\phi\sin\theta - \cos\phi\sin\psi & \sin\phi\sin\theta\sin\psi + \cos\phi\cos\psi & \sin\phi\cos\theta \\ \cos\phi\sin\theta\cos\psi + \sin\phi\sin\psi & \cos\phi\sin\theta\sin\psi - \sin\phi\cos\psi & \cos\phi\cos\theta \end{pmatrix} \quad (1)$$

3.1.2. System Model Establishment

Quaternions are used for describing changes in heading and attitude due to their singularity-free nature and low computational requirements [7]. Gyroscope data is used for quaternion updates, while accelerometer and magnetometer measurements provide observed values.

(1) Attitude Estimation Based on Accelerometer

The accelerometer outputs the body acceleration. The gravitational acceleration in the navigation frame is $g_n = (0,0,g)^T$, and the output of the accelerometer in the body frame is$a_b = \left(a_x, a_y, a_z\right)^T$. The transformation relationship is:

$$\begin{pmatrix} a_x \\ a_y \\ a_z \end{pmatrix} = C_n^b \begin{pmatrix} 0 \\ 0 \\ g \end{pmatrix} = \begin{pmatrix} -g\sin\theta \\ g\cos\theta\sin\phi \\ g\cos\theta\cos\phi \end{pmatrix} \quad (2)$$

From the accelerations obtained by the above formula, the pitch and roll angles can be derived as:

$$\begin{cases} \theta = -\arcsin\left(\frac{a_x}{g}\right) \\ \phi = \arctan\left(\frac{a_y}{a_z}\right) \end{cases} \quad (3)$$

(2) Attitude Estimation Based on Magnetometer

The magnetometer outputs the geomagnetic field vector. On the Earth's surface, the geomagnetic field typically points toward magnetic north, consisting of a northward component and a vertical component, but no eastward component. Therefore, the magnetic field vector in the geomagnetic coordinate system can be expressed as $(N, 0, D)$. When the geomagnetic coordinate system coincides with the navigation frame n, $m_n = (M, 0, M_0)$ represents the magnetometer output in the navigation frame. Assuming the magnetometer output in the body frame b is $m_n = \left(m_x, m_y, m_z\right)^T$, it can be transformed using the transformation matrix C_n^b as follows:

$$m_b = C_n^b m_n \quad (4)$$

After simplification, this becomes:

$$\begin{pmatrix} m_x \\ m_y \\ m_z \end{pmatrix} = \begin{pmatrix} M\,cos\,\theta\,cos\,\psi_m - M_0\,sin\,\theta \\ M\,cos\,\theta\,sin\,\psi_m \\ M\,sin\,\theta + M_0\,cos\,\theta \end{pmatrix} \tag{5}$$

Thus, the horizontal component of the geomagnetic vector is:

$$\begin{pmatrix} M\,cos\,\theta\,cos\,\psi_m - M_0\,sin\,\theta \\ M\,cos\,\theta\,sin\,\psi_m \end{pmatrix} \tag{6}$$

The yaw angle can then be calculated as:

$$\psi_m = arctan\left(\frac{m_y}{m_x}\right) \tag{7}$$

Finally, the magnetic yaw angle is given by:

$$\psi_{mag} = \psi_m + \alpha \tag{8}$$

Where $\alpha$is the magnetic declination, correcting the angle difference between magnetic north and true north. This method uses geomagnetic information from the magnetometer, applying a mathematical model and coordinate transformation to accurately estimate the UAV's yaw angle.

(3) Attitude Estimation Based on Gyroscope

The gyroscope outputs the angular acceleration of the sensitive carrier. The dynamic model update of gyroscope angular velocity based on quaternions can be expressed as:

$$\dot{q} = \frac{1}{2} q \otimes \omega^b \tag{9}$$

Where $\omega^b = (\omega_x, \omega_y, \omega_z)$ represents the angular velocity measured by the gyroscope, and $q = (q_0, q_1, q_2, q_3)^T$ represents the attitude quaternion. The matrix form of equation (10) can be expressed as:

$$\begin{pmatrix} \dot{q}_0 \\ \dot{q}_1 \\ \dot{q}_2 \\ \dot{q}_3 \end{pmatrix} = \frac{1}{2} \begin{pmatrix} 0 & -\omega_x & -\omega_y & -\omega_z \\ \omega_x & 0 & \omega_z & -\omega_y \\ \omega_y & -\omega_z & 0 & \omega_x \\ \omega_z & \omega_y & -\omega_x & 0 \end{pmatrix} \begin{pmatrix} q_0 \\ q_1 \\ q_2 \\ q_3 \end{pmatrix} \tag{10}$$

Using the Picard iterative method to solve the quaternion differential equation (9), its discrete form is given by:

$$q(t_k) = \left[cos\left(\frac{\Delta\varphi}{2}\right) + sin\left(\frac{\Delta\varphi}{2}\right)\frac{\Delta\Omega}{\Delta\varphi}\right] q(t_{k-1}) \tag{11}$$

Where $\triangle\,\varphi = \sqrt{\alpha_x^2 + \alpha_y^2 + \alpha_z^2}$ is the angular increment during the sampling interval $[tk-1, tk]$, $\alpha_i = \int_{t_{k-1}}^{t_k} \omega_{\,i} dt, i = x, y, z$, and $\triangle\,\Omega = (\alpha_x\ \alpha_y\ \alpha_z)^T$.

The transformation matrix from the body frame to the navigation frame, represented using quaternions, is given by:

$$C_n^b = \begin{pmatrix} q_0^2 + q_1^2 - q_2^2 - q_3^2 & 2(q_1q_2 + q_0q_3) & 2(q_1q_3 - q_0q_2) \\ 2(q_1q_2 - q_0q_3) & q_0^2 - q_1^2 + q_2^2 - q_3^2 & 2(q_2q_3 + q_0q_1) \\ 2(q_1q_3 + q_0q_2) & 2(q_2q_3 - q_0q_1) & q_0^2 - q_1^2 - q_2^2 + q_3^2 \end{pmatrix} \tag{12}$$

Thus, the UAV attitude angles can be expressed using quaternions as:

$$\begin{cases} \phi = arctan\left(\frac{2(q_0q_1+q_2q_3)}{q_0^2-q_1^2-q_2^2+q_3^2}\right) \\ \theta = arcsin(2(q_0q_2-q_1q_3)) \\ \psi = arctan\left(\frac{2(q_0q_3+q_1q_2)}{q_0^2+q_1^2-q_2^2-q_3^2}\right) \end{cases} \tag{13}$$

3.2. Accelerometer Correction Model

3.2.1. Model Structure

Based on the previously correctly established navigation frame and body frame, we develop an accelerometer correction model to adjust the output values of the accelerometer. The structure of the model is illustrated in Fig 1.

As shown in Fig. 1, the Kalman filter uses the difference between the corrected accelerometer output and the gravitational acceleration in the body frame as its measurement. After filtering, the attitude angle error and non-gravitational acceleration error are obtained, correcting the coordinate transformation matrix. Non-gravitational acceleration is derived from both the Kalman filter and GPS velocity.

The Kalman filter provides an estimated non-gravitational acceleration at the accelerometer's frequency, maintaining short-term stability. However, error accumulation reduces its long-term accuracy. Conversely, the GPS-derived non-gravitational acceleration, while stable and reliable, has a lower update frequency and cannot correct accelerometer outputs timely. Therefore, this study designs an accelerometer correction model that combines both sources of non-gravitational acceleration to ensure accurate and stable attitude estimation.

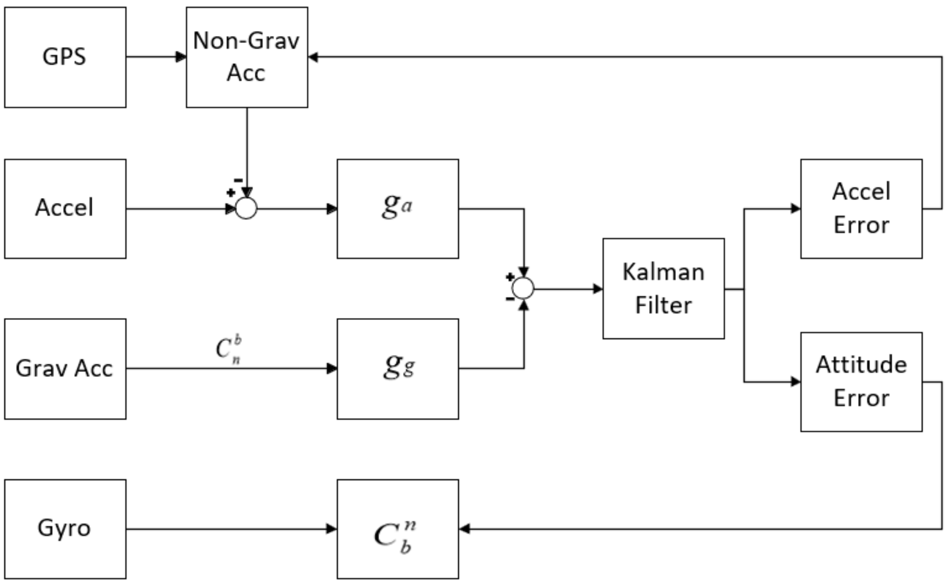

Figure 1. Acceleration correction model block diagram

3.2.2. Estimating Non-Gravitational Acceleration

To obtain the attitude angle error and non-gravitational acceleration error as state variables, the system state variables are defined as follows:

$$X_\varepsilon = [\theta_\varepsilon \quad a_b^\xi]^T \tag{14}$$

Where the attitude angle error is given by: $\theta_\varepsilon = \begin{bmatrix} \theta_{\varepsilon x} \\ \theta_{\varepsilon y} \\ \theta_{\varepsilon z} \end{bmatrix}$ and the non-gravitational acceleration error is given by: $a_{b\varepsilon} = \begin{bmatrix} a_{b\varepsilon x} \\ a_{b\varepsilon y} \\ a_{b\varepsilon z} \end{bmatrix}$. The system state equation can be expressed as:

$$X_{\varepsilon,k} = \Phi_{k,k-1} X_{\varepsilon,k-1} + w_k \tag{15}$$

Where $\Phi_{k,k-1}$ represents the state transition matrix and w_k is the process noise.

In the acceleration correction model, the current non-gravitational acceleration error and attitude angle error have been corrected. The state variables at adjacent time steps are uncorrelated, and the state transition matrix can be expressed as: $\Phi_{k,k-1} = 0_{6\times6}$. Therefore, the state one-step prediction equation and state estimation equation in the Kalman filter are simplified as follows:

$$\hat{X}_{\varepsilon,k|k-1} = 0 \tag{16}$$

$$\hat{X}_{\varepsilon,k} = \hat{X}_{\varepsilon,k|k-1} + K_k(Z_{\varepsilon,k} - H_k \hat{X}_{\varepsilon,k|k-1}) = K_k Z_{\varepsilon,k} \tag{17}$$

Where $Z_k$represents the measurement information at the current time step, H_k is the measurement matrix, and K_k is the Kalman filter gain matrix at the current time step.

The corrected acceleration, obtained by removing the estimated non-gravitational acceleration interference from the raw accelerometer values, is denoted as $\hat{g}^b{}_{a,k}$:

$$\hat{g}^b{}_{a,k} = -f_k^b + \hat{a}^b{}_{k-1} \tag{18}$$

Where f_k^b is the raw accelerometer value and $\hat{a}^b{}_{k-1}$ is the estimated non-gravitational acceleration.

The standard gravitational acceleration in the body frame, $\hat{g}_{g.k}^b$, can be expressed as:

$$\hat{g}_{g.k}^b = \hat{C}_{n,k}^b g^n \tag{19}$$

Where g^n represents the local gravitational acceleration in the navigation frame, and $\hat{C}_{n,k}^b$ is the coordinate transformation matrix from the navigation frame to the body frame at time k.

The difference between $\hat{g}_{a,k}^b$ and $\hat{g}_{g,k}^b$is taken as the measurement information $Z_{\varepsilon,k}$:

$$Z_{\varepsilon,k} = \hat{g}_{a,k}^b - \hat{g}_{g,k}^b \tag{20}$$

Expanding equation (7) yields:

$$Z_{\varepsilon,k} = \hat{g}_{a,k}^b - \hat{g}_{g,k}^b = \Delta R(-\hat{\theta}_{\varepsilon,k})\hat{g}_{g,k}^b + \hat{a}_{\varepsilon,k}^b - v_{a,k} - \hat{g}_{g,k}^b = (\hat{g}_{g,k}^b \times)\theta_{\varepsilon,k} + \hat{a}_{b\varepsilon,k} - v_{a,k} \tag{21}$$

Where $R(\,)$ denotes the small-angle rotation matrix.

The system measurement equation can be expressed as:

$$Z_{\varepsilon,k} = H_{\varepsilon,k}X_{\varepsilon,k} + v_{\varepsilon,k} = H_{\varepsilon,k}\begin{bmatrix}\theta_{\varepsilon,k} \\ a^b_{\varepsilon,k}\end{bmatrix} + v_{\varepsilon,k} \tag{22}$$

Where $v_{\varepsilon,k}$ represents the measurement noise, with variance denoted as R_k, and the measurement matrix $H_{\varepsilon,k}$ is expressed as follows:

$$H_{\varepsilon,k} = \left[\left(\hat{g}^g_b, k\times\right) \quad I_{3\times3}\right] \tag{23}$$

The filter gain matrix is:

$$P_{k/k-1} = \Phi_{k,k-1}P_{k-1}\Phi_{k,k-1} + Q_k = Q_k \tag{24}$$

One-step prediction mean square error:

$$K_k = P_{k/k-1}H^T_{\varepsilon,k}(H_{\varepsilon,k}P_{k/k-1}H^T_{\varepsilon,k} + R_k)^{-1} \tag{25}$$

Estimated mean square error:

$$P_k = (I - K_kH_{\varepsilon,k})P_{k/k-1} \tag{26}$$

Based on the obtained state error estimate $\hat{X}_{\varepsilon,k}$, the estimated non-gravitational acceleration at time $\theta_{\varepsilon,k}$, using the updated attitude transition matrix C^n_b, k and attitude angle error $\hat{a}^b_k$, can be expressed as:

$$\hat{a}^b_k = \hat{a}^b_{k-1} - \hat{a}^b_{\varepsilon,k} \tag{27}$$

3.3. External Non-Gravitational Acceleration

The external non-gravitational acceleration is calculated using the velocity information provided by GPS and is used to correct the accelerometer's raw values. The GPS output signal has a period of T_2, while the accelerometer output signal has a period of T_1. Denote the velocity information in the navigation frame at time k as $v^n_{g,k}$. The external non-gravitational acceleration $a^n_{g,k}$ at time $k$in the navigation frame is given by:

$$a^n_{g,k} = \frac{v^n_{g,k} - v^n_{g,k-1}}{T_2} \tag{28}$$

The external non-gravitational acceleration $a^n_{g,k}$ is then transformed from the navigation frame to the body frame:

$$a^b_{g,k} = C^n_b a^n_{g,k} \tag{29}$$

Typically, the GPS period T_2 is an integer multiple of the accelerometer period T_1, represented as T_2=nT1T_2 = nT1.

The raw accelerometer values over the period T_2 are integrated to obtain the average raw accelerometer value during this time period:

$$f^b_{a,k} = \frac{1}{n}\sum_{i=1}^{n} f_b^{k+iT_1} \tag{30}$$

Through the above derivation, the corrected accelerometer output $g^b_{o,k}$ after the external non-gravitational acceleration correction can be expressed as:

$$g_{o,k}^b = f_{a,k}^b - a_{g,k}^b \tag{31}$$

4. RESULTS AND DISCUSSION

4.1. Data Collection for Experiments

In this simulation, we used MATLAB Simulink to create a sensor fusion model for accurate vehicle attitude and position estimation along a circular path. The model integrated accelerometer, gyroscope, magnetometer, and GPS data at 100Hz, with initial conditions set by a 28-dimensional vector. Quaternions captured attitude changes, while an asynchronous sensor fusion filter processed measurement errors. Dynamic data and real-time monitoring ensured comprehensive analysis and visualization, highlighting the model's accuracy and effectiveness. This robust setup demonstrated the system's stability and noise levels, validating the model's performance and potential in complex dynamic environments.

Figure 2 illustrates the comprehensive sensor data and trajectory analysis, highlighting the model's effectiveness and accuracy in vehicle dynamics estimation.

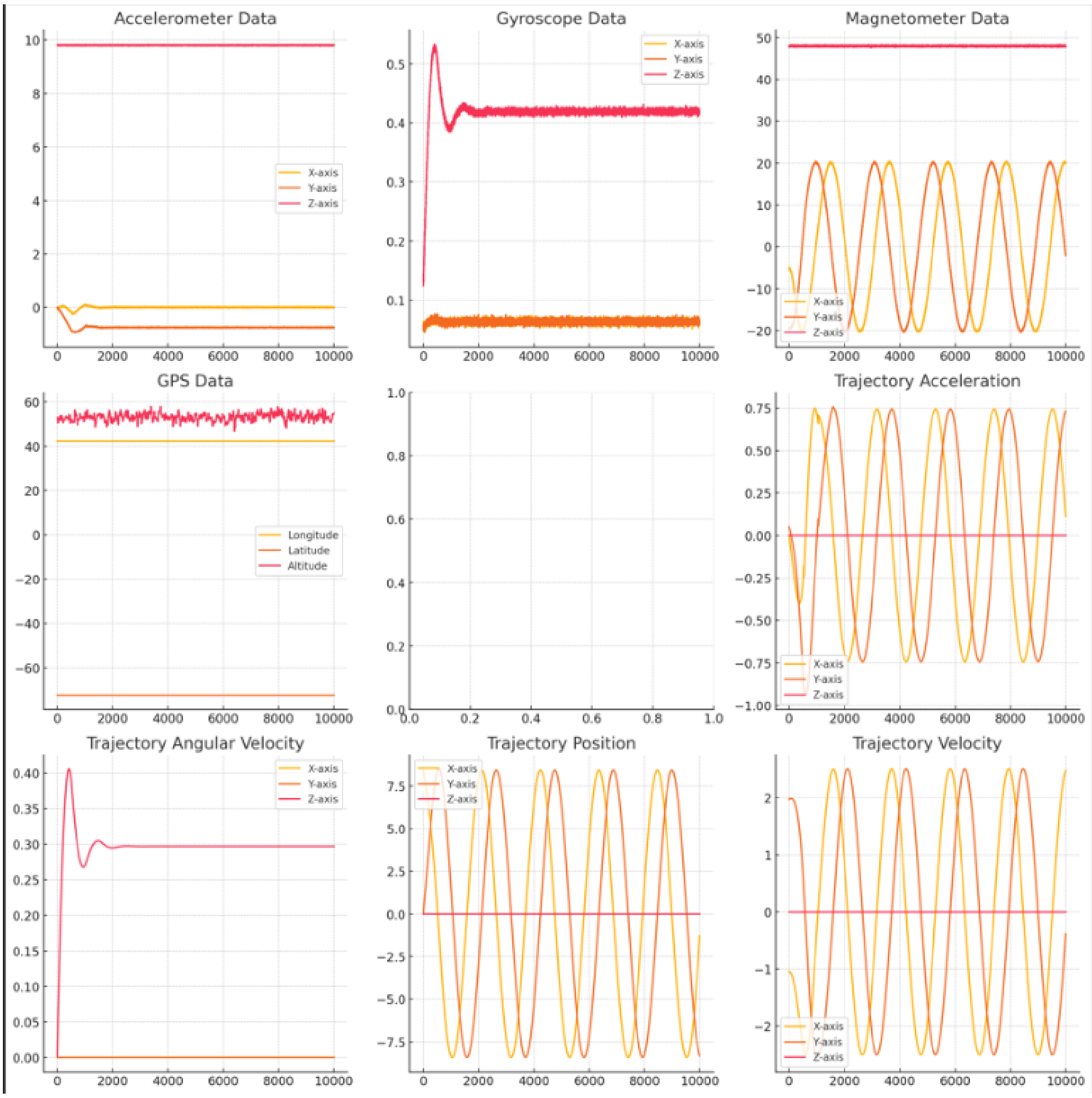

Figure 2. The comprehensive sensor data and trajectory analysis

4.2. Verification of the Accelerometer Correction Model

4.2.1. Using Only Accelerometers

In this phase, we verify the accelerometer correction model without GPS. We analyze the impact of relying solely on accelerometer data for attitude estimation over time, as shown in Figures 3 and 4.

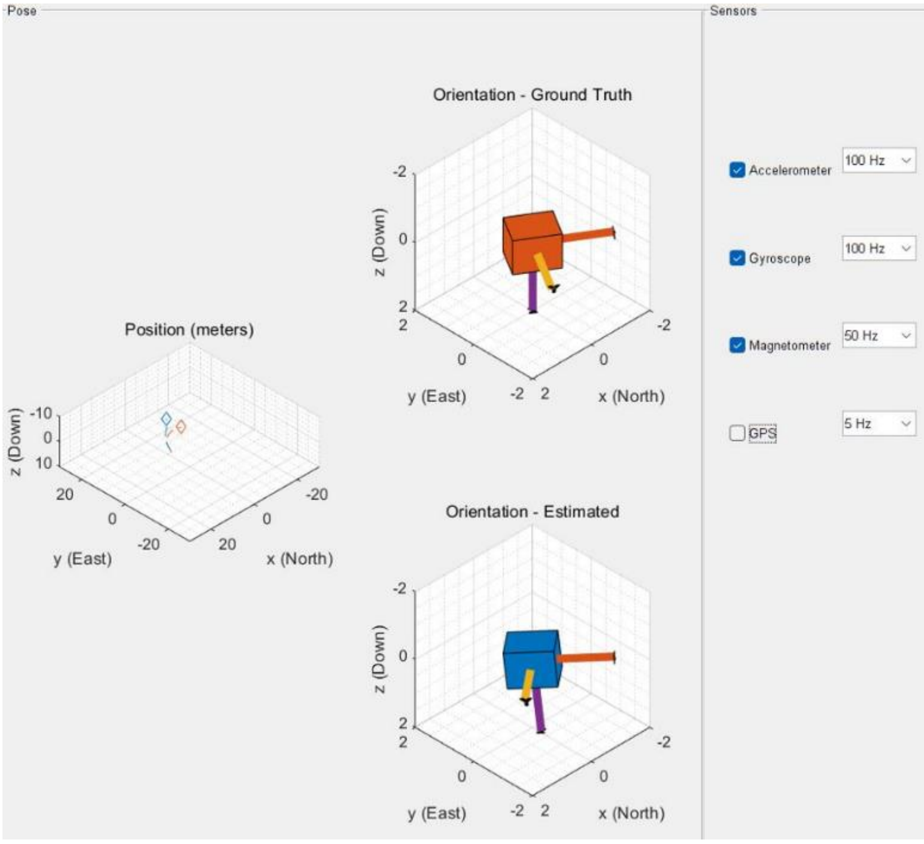

Figure 3. 3D Visualization

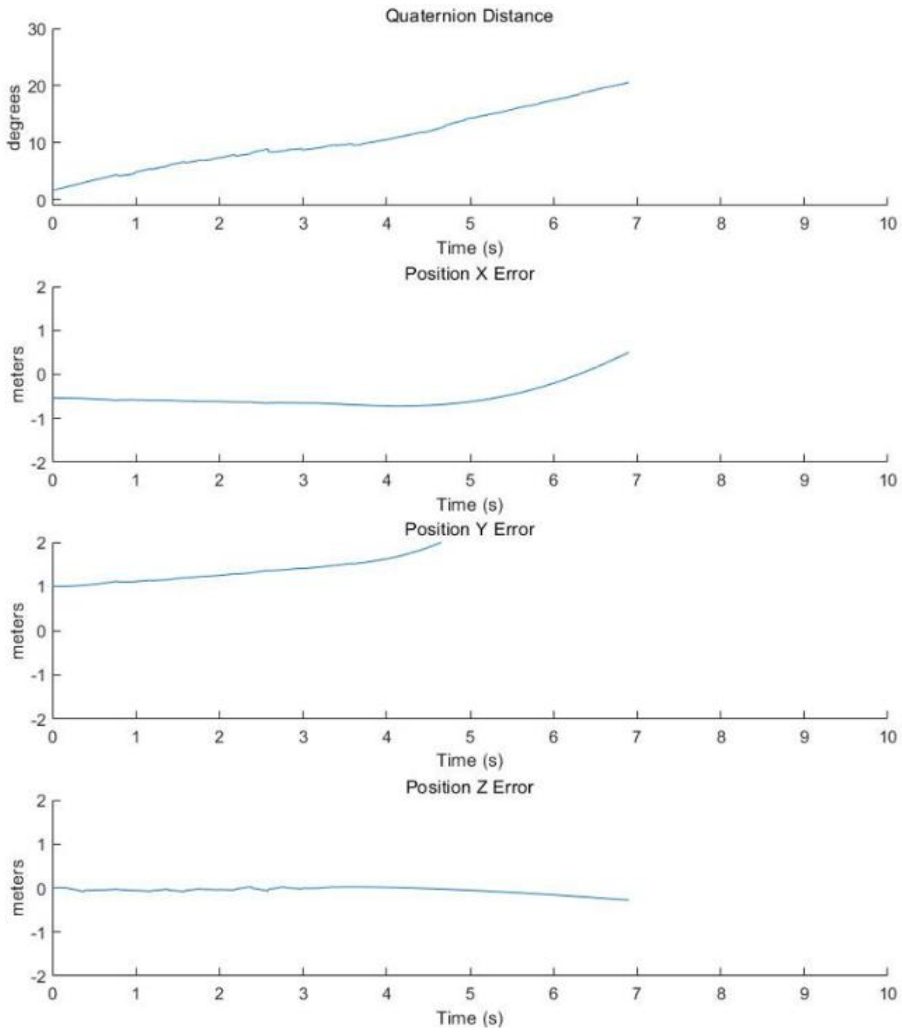

Figure 4. Error Analysis

Figure 3 (3D Visualization) displays the vehicle's 3D position and compares true and estimated orientations using accelerometer data alone.

Figure 4 (Error Analysis) shows the angular distance between true and estimated orientations (Quaternion Distance) and position errors over time.

Attitude Instability: Figure 3 indicates significant deviations over time, showing unstable attitude estimation with only accelerometers.

Error Accumulation: Figure 4 demonstrates rapid growth in orientation errors due to sensor noise and bias. Position Errors: Figure 4 also reveals increasing position errors, highlighting unreliability without GPS corrections.

This experiment emphasizes the limitations of relying solely on accelerometer data. Over time, sensor inaccuracies lead to significant orientation and position errors. Integrating GPS is essential for accurate, stable estimations, crucial for robust navigation systems in dynamic environments.

4.2.2. Using GPS without Accelerometers

In this phase, we examine the effects of using GPS alone for position and attitude corrections without accelerometer data. The goal is to assess how well GPS maintains stable estimates of vehicle dynamics over time, as shown in Figures 5 and 6.

Figure 5 (3D Visualization) displays the vehicle's 3D position and compares true and estimated orientations using GPS data alone. Figure 6 (Error Analysis) shows the angular distance between true and estimated orientations (Quaternion Distance) and position errors over time.

Initial Stability: Figure 5 shows stable initial estimates due to accurate GPS data.

GPS Update Rate Limitation: Figure 6 reveals increasing orientation and position errors over time, indicating the 5Hz GPS update rate is insufficient for capturing rapid vehicle dynamics.

Error Trends: The system struggles to maintain accurate estimates during complex movements due to the low GPS update rate.

Using GPS alone highlights challenges in dynamic environments. Initial estimates are stable, but errors grow as GPS can't update frequently enough. Integrating high-frequency sensors like accelerometers and gyroscopes is essential to complement GPS and ensure robust, accurate real-time estimations. Combining GPS and IMU data is crucial for high accuracy in vehicle navigation systems.

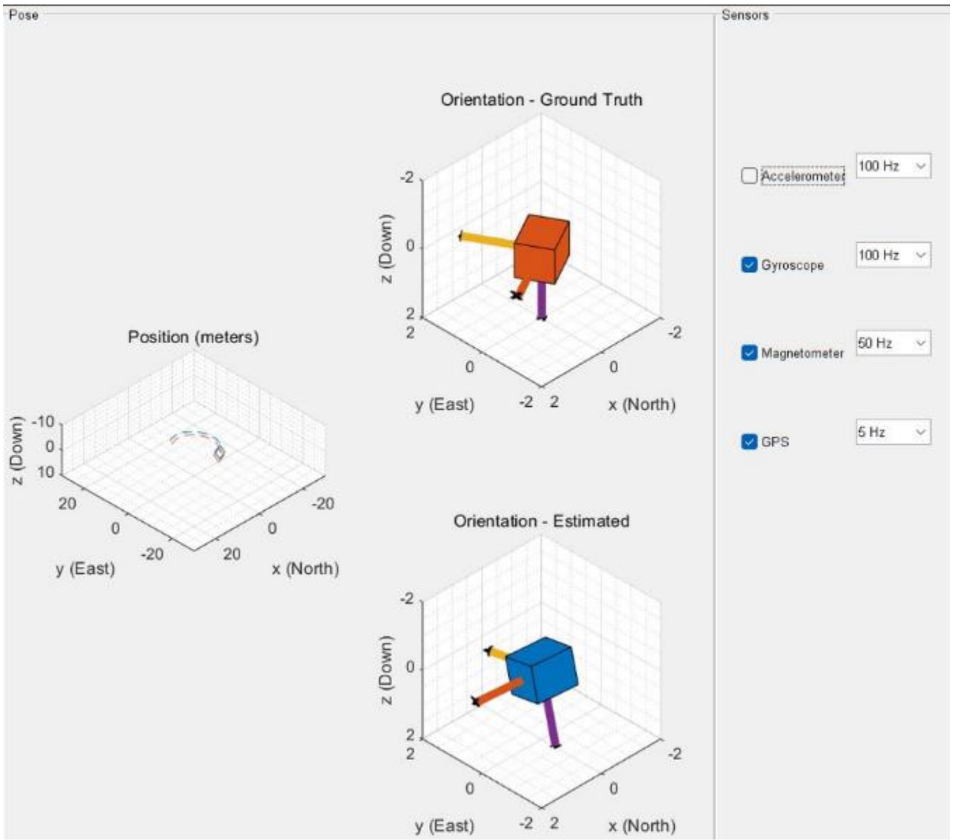

Figure 5. 3D Visualization

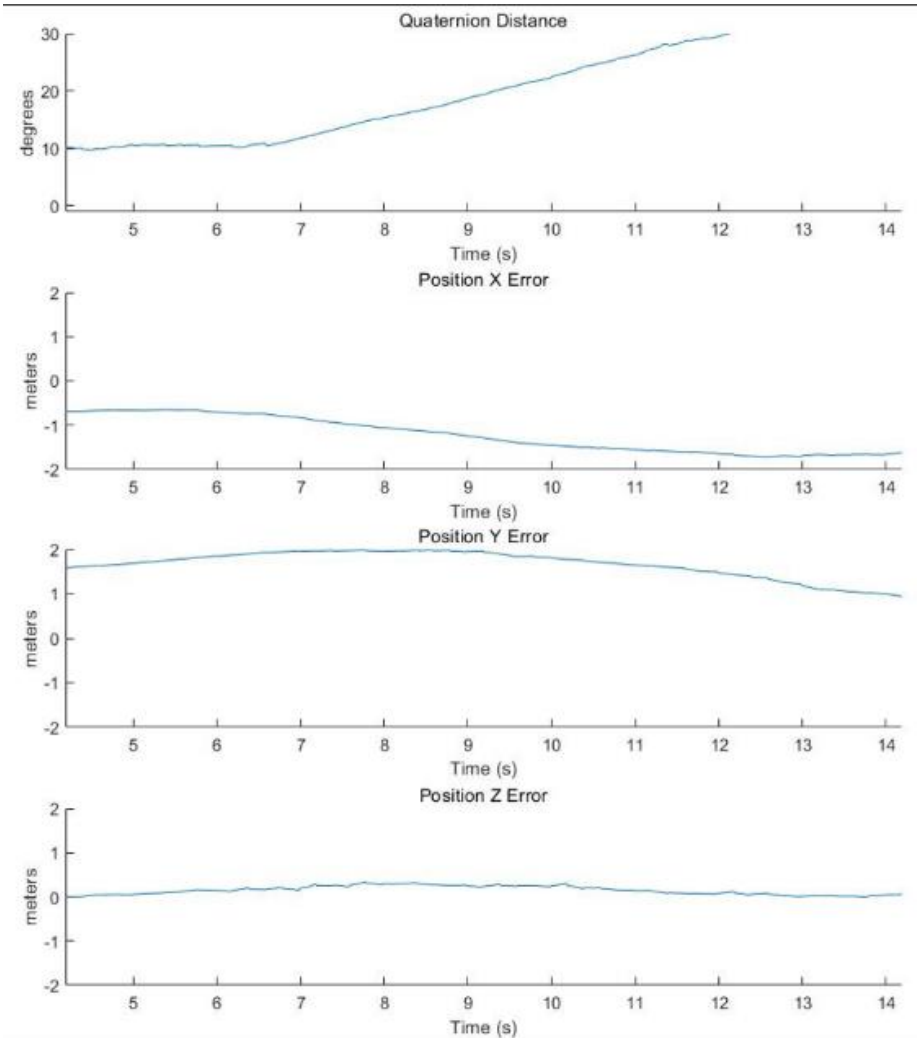

Figure 6. Error Analysis

4.2.3. Application of the Accelerometer Correction Model

In this phase, we investigate the effects of fusing GPS and accelerometer data using a Kalman filter to enhance attitude and position estimation. The goal is long-term stability in the vehicle's orientation and position via the accelerometer correction model. The results are depicted in Figures 7 and 8.

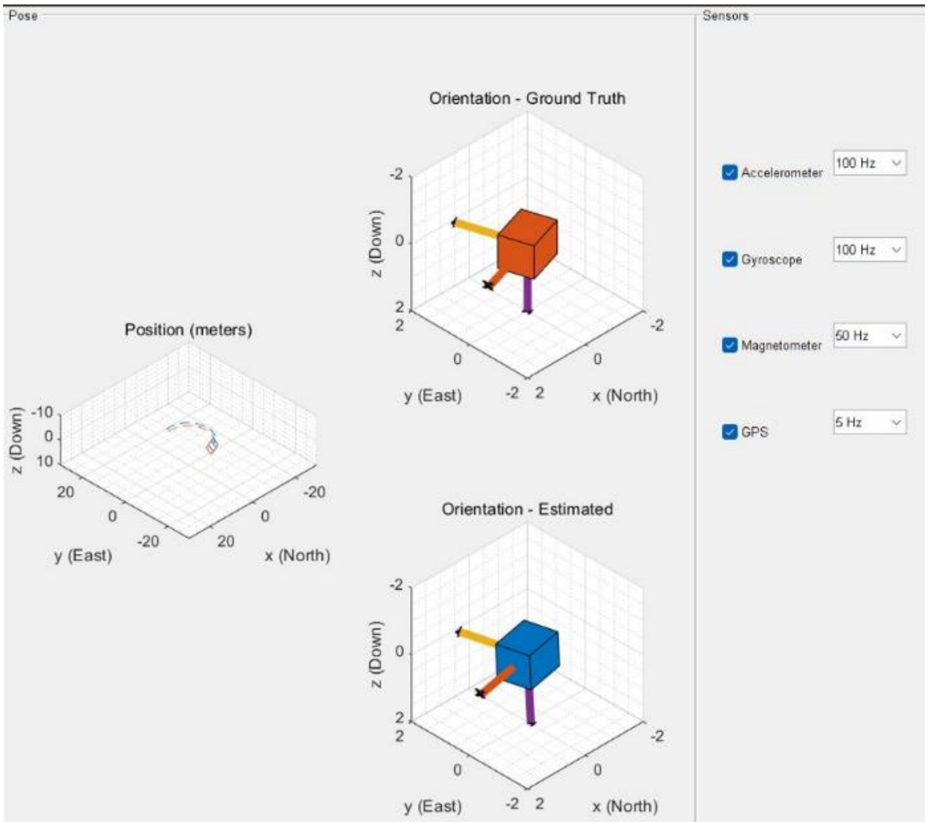

Figure 7. 3D Visualization

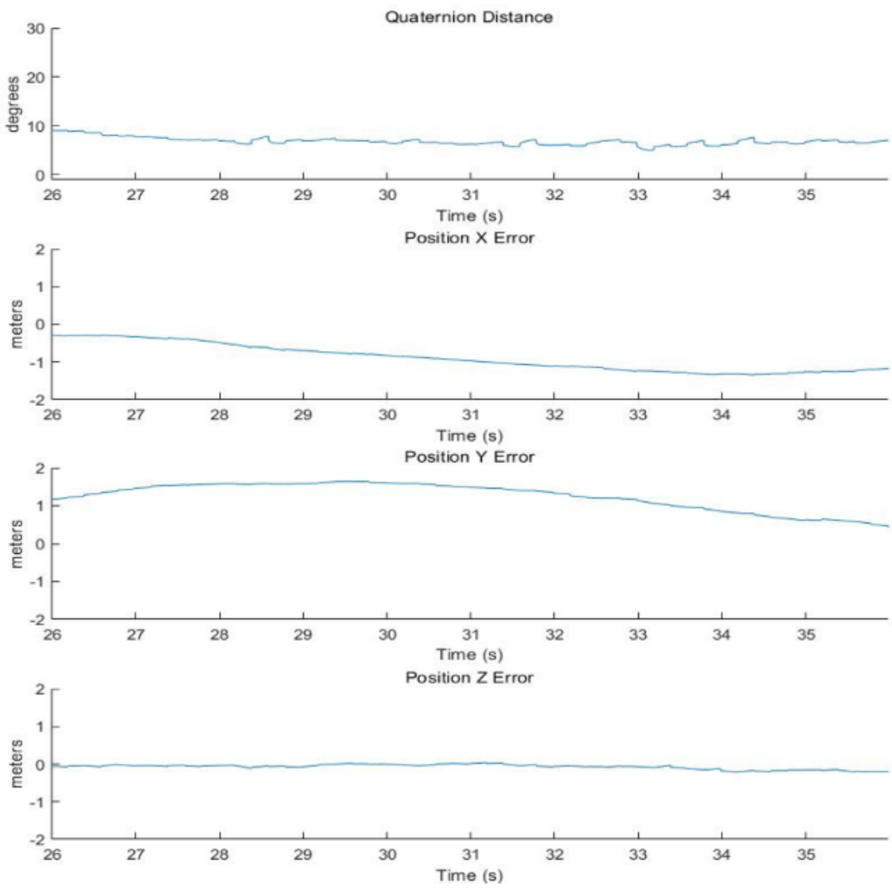

Figure 8. Error Analysis

Figure 7 (3D Visualization): This plot shows the vehicle's 3D position and compares true and estimated orientations using fused GPS and accelerometer data.

Figure 8 (Error Analysis): This plot illustrates the angular distance between true and estimated orientations (Quaternion Distance) and position errors along the x, y, and z axes over time.

Enhanced Stability: Figure 7 shows stable and accurate attitude estimation from the data fusion.

Reduced Error Accumulation: Figure 8 demonstrates that orientation errors remain small and stable, showing effective error mitigation by the Kalman filter.

Improved Position Accuracy: Figure 8 shows minor and consistent position errors, indicating improved accuracy through data fusion.

The integration of GPS and accelerometer data, processed through a Kalman filter, significantly enhances the stability and accuracy of attitude and position estimations. This method effectively combines high-frequency updates from accelerometers with precise GPS data, addressing limitations of using each sensor independently. The results highlight the effectiveness of sensor fusion in developing robust and reliable navigation systems, maintaining high accuracy over extended periods in dynamic environments. This validation supports advanced filtering techniques for optimizing integrated sensor system performance in practical applications.

5. CONCLUSION

This research successfully implements and validates an advanced accelerometer correction model using MATLAB Simulink to enhance UAV attitude and position estimation in dynamic environments. By integrating GPS and accelerometer data through a Kalman filter, our model overcomes the limitations of traditional methods. It provides robust and precise long-term estimates, mitigating noise and biases from individual sensors. Simulation results show that combining high-frequency accelerometer updates with GPS data significantly improves accuracy and stability over extended periods, outperforming methods that use only GPS or accelerometers. This study highlights the importance of sensor fusion in modern navigation, offering a cost-effective solution for low-cost UAV systems.

ACKNOWLEDGEMENTS

I sincerely thank the scholars whose research in attitude estimation and sensor fusion laid a solid foundation for this study. My deepest gratitude goes to my advisor for his patient guidance and invaluable support. I also appreciate my fellow students for their assistance in experiment design, data processing, and thesis writing. Thank you all!

REFERENCES

[1] LEFFERTS E J, MARKLEY F L, SHUSTER M D. Kalman filtering for spacecraft attitude estimation [J]. Journal of Guidance, Control and Dynamics, 2012, 5(4): 536-542.

[2] Lu Yanjun, Chen Yuhuo, Zhang Xiaodong, et al. Research on Attitude Information Fusion Method Based on Extended Kalman Filter [J]. Journal of Instrumentation, 2020, 41(9): 281-288.

[3] Cui Peilin, Zhou Xiang, Lv Jing, et al. Adaptive Error Quaternion Unscented Kalman Filter Attitude Solution Method for Quadrotor UAV [J]. Journal of Xi'an Jiaotong University, 2019, 53(3): 97-110.

[4] KHAMSEH H B, JANABI-SHARIFI F. UKF-based LQR control of a manipulating unmanned aerial vehicle [J]. Unmanned Systems, 2017, 5(3): 131-139.

[5] GARCIA R V, KUGA H K, SILVA W R, et al. Unscented Kalman filter and smoothing applied to attitude estimation of artificial satellites [J]. Computational & Applied Mathematics, 2018, 37(4): 55-64.

[6] WANG G Q, LI N, ZHANG Y G. Hybrid consensus signal filtering for attitude estimation filter using statistical linearization [J]. Transactions of the Institute of Measurement and Control, 2017, 40: 2517-2525.

[7] Liu Xingchuan, Zhang Sheng, Li Lizhe, et al. Quaternion-Based Attitude Measurement Algorithm for MARG Sensors [J]. Journal of Tsinghua University (Natural Science Edition), 2012, 52(5): 627-631.